

QCD sum rules with spectral densities solved in inverse problemsHsiang-nan Li  and Hiroyuki Umeeda *Institute of Physics, Academia Sinica, Taipei, Taiwan 115, Republic of China*

(Received 25 August 2020; accepted 10 November 2020; published 8 December 2020)

We construct QCD sum rules for nonperturbative studies without assuming the quark-hadron duality for the spectral density at low energy on the hadron side. Instead, both resonance and continuum contributions to the spectral density are solved with the operator-product-expansion input on the quark side by treating sum rules as an inverse problem. This new formalism does not involve the continuum threshold, does not require the Borel transformation and stability analysis, and can be extended to extract properties of excited states. Taking the two-current correlator as an example, we demonstrate that the series of ρ resonances can emerge in our formalism, and the decay constants $f_{\rho(770)}(f_{\rho(1450)}, f_{\rho(1700)}, f_{\rho(1900)}) \approx 0.22$ (0.19, 0.14, 0.14) GeV for the masses $m_{\rho(770)}(m_{\rho(1450)}, m_{\rho(1700)}, m_{\rho(1900)}) \approx 0.78$ (1.46, 1.70, 1.90) GeV are determined. We also show that the decay width $\Gamma_{\rho(770)} \approx 0.17$ GeV can be obtained by substituting a Breit-Wigner parametrization for the $\rho(770)$ pole on the hadron side. It is observed that quark condensates of dimension-six on the quark side are crucial for establishing those ρ resonances. Handling the conventional sum rules with the duality assumption as an inverse problem, we find that the multiple pole sum rules widely adopted in the literature do not describe the ρ excitations reasonably. The precision of our theoretical outcomes can be improved systematically by including higher-order and higher-power corrections on the quark side. Broad applications of this formalism to abundant low energy QCD observables are expected.

DOI: [10.1103/PhysRevD.102.114014](https://doi.org/10.1103/PhysRevD.102.114014)**I. INTRODUCTION**

QCD sum rules have become one of the major non-perturbative approaches to low energy hadronic processes, since they were proposed decades ago [1]. This approach relies heavily on the assumption of the quark-hadron duality for the spectral density on the hadron side in a low energy region, whose theoretical uncertainty is difficult to control and quantify. The Borel transformation is applied to suppress model dependent continuum contributions on the hadron side and higher power corrections on the quark side. Nevertheless, the typical scale of a Borel mass may not be large enough for justifying the desired suppression. The choice of the continuum threshold is a bit arbitrary, though the stability criterion, i.e., the existence of the so-called “sum rule window” under the variation of the continuum threshold and Borel mass, has been imposed. However, the above prescriptions are quite discretionary [2], such that a strong dependence on the continuum threshold and Borel mass is not avoidable. Besides, one usually invokes the vacuum saturation hypothesis (factorization) to replace higher dimension condensates with

products of lower dimension ones on the quark side, which also causes uncertainty. Therefore, there has been concern on the rigorousness and predictive power of QCD sum rules [3,4].

In this paper, we will handle QCD sum rules in a different way, attempting to resolve the aforementioned difficulty to some extent. The spectral density on the hadron side of a sum rule, including both resonance and continuum contributions, is regarded as an unknown. The operator product expansion (OPE) on the quark side is calculated in the standard way. A sum rule is then treated as an inverse problem, in which the unknown (source distribution) is solved from the OPE input (potential observed outside the distribution). This formalism does not involve the continuum threshold because the continuum can be a smooth distribution not related to the perturbative spectral density. It does not require a Borel transformation to suppress the continuum contribution, which will be solved from the inverse problem. The suppression on the higher power corrections can be achieved by considering the input in the deep euclidean region. Once the unknown spectral density is solved directly, the stability criterion for a conventional sum rule is not necessary. Certainly, the Borel transformation can be applied to our formalism, but it will be verified that results from the versions with and without this transformation are similar.

It has been known that an inverse problem is ill-posed and allows for the existence of multiple solutions. We will

Published by the American Physical Society under the terms of the Creative Commons Attribution 4.0 International license. Further distribution of this work must maintain attribution to the author(s) and the published article's title, journal citation, and DOI. Funded by SCOAP³.

show that the existence of multiple solutions grants the extension of our formalism to studies of excited states, which impose a challenge to conventional sum rules. Taking the two-current correlator as an example, we demonstrate how to obtain the masses and decay constants of the ρ resonances. We first fix the correction to the vacuum saturation hypothesis for higher dimension condensates on the quark side from the input of the ground state $\rho(770)$ mass and determine the $\rho(770)$ meson decay constant by solving the sum rule as an inverse problem. The lower state observables are then adopted as inputs to extract properties of higher states one by one. A series of (radial) excitations can be probed systematically following the above strategy. The masses $m_{\rho(770)}(m_{\rho(1450)}, m_{\rho(1700)}, m_{\rho(1900)}) \approx 0.78$ (1.46, 1.70, 1.90) GeV and the decay constants $f_{\rho(770)}(f_{\rho(1450)}, f_{\rho(1700)}, f_{\rho(1900)}) \approx 0.22$ (0.19, 0.14, 0.14) GeV are extracted. Besides, the decay width $\Gamma_{\rho(770)} \approx 0.17$ GeV is also derived by substituting a Breit-Wigner parametrization for the $\rho(770)$ pole on the hadron side. To understand how the nonperturbative condensates influence the appearance of the ρ resonance, we examine the impacts from power corrections of various dimensions. It is found that the quark condensate of dimension-six plays a crucial role for establishing the $\rho(770)$ state.

Properties of excited states have been investigated in conventional QCD sum rules by employing the double pole plus continuum model for a spectral density [5–10]. The second pole for the excited state was put in by hand, and *ad hoc* prescriptions for choosing an appropriate continuum threshold have to be postulated [11], such as the lower bound of the continuum threshold being set to the excited state mass plus 100 MeV. Treating the above conventional sum rules as an inverse problem, we explicitly show that there are no signs for excited ρ resonances, once the quark-hadron duality is assumed. This investigation casts doubt on the multiple pole QCD sum rules, which have been widely adopted in the literature. Our formalism is close to the Bayesian approach to QCD sum rules [4], in which the specific form of the spectral density was not assumed but derived using the maximum entropy method. Though it is possible to explore the existence of excited states by applying this method to sum rules, at least its application to the nucleon mass spectrum has not been successful [12]. We suspect that the failure is attributed to the ill-posed essence of an inverse problem, which makes difficult searching for correct excitations from many allowed solutions without any specific parametrization for the spectral density. Hence, our work provides a justified and practical approach to studies of excited states based on QCD sum rules.

The rest of the paper is organized as follows. In Sec. II, we construct our formalism starting from the dispersion relation for a two-current correlator. The distinction from conventional QCD sum rules, namely, no assumption of the

quark-hadron duality, is highlighted. We elaborate the extractions of the masses and decay constants of the series of ρ resonances by solving the sum rules as an inverse problem in Sec. III, starting with the $\rho(770)$ meson mass, which is used to fix the factorization violation parameter associated with the dimension-six condensate. We end the search for the ρ excitations at $\rho(2000)$ in our formalism, for which theoretical and experimental studies are still rare. The conventional multiple pole sum rules with the duality assumption are also solved in a similar way to confirm our concern about their applications to excited states. Section IV contains the conclusion and outlooks.

II. FORMALISM

The series of ρ resonances is one of the first objects analyzed in QCD sum rules, through which we formulate our approach and demonstrate its application. We first briefly recollect the idea of conventional QCD sum rules, starting with the two-point correlator,

$$\begin{aligned} \Pi_{\mu\nu}(q^2) &= i \int d^4x e^{iq \cdot x} \langle 0 | T [J_\mu(x) J_\nu(0)] | 0 \rangle \\ &= (q_\mu q_\nu - g_{\mu\nu} q^2) \Pi(q^2), \end{aligned} \quad (1)$$

for the current $J_\mu = (\bar{u}\gamma_\mu u - \bar{d}\gamma_\mu d)/\sqrt{2}$. The vacuum polarization function $\Pi(q^2)$ obeys the identity,

$$\Pi(q^2) = \frac{1}{2\pi i} \oint ds \frac{\Pi(s)}{s - q^2}, \quad (2)$$

where the contour, depicted in Fig. 1, consists of two pieces of horizontal lines above and below the positive horizontal axis, i.e., the branch cut, and a circle of large radius R . For s far away from physical poles, the perturbative evaluation of $\Pi(s)$ is reliable, so the right-hand side of Eq. (2) can be written as

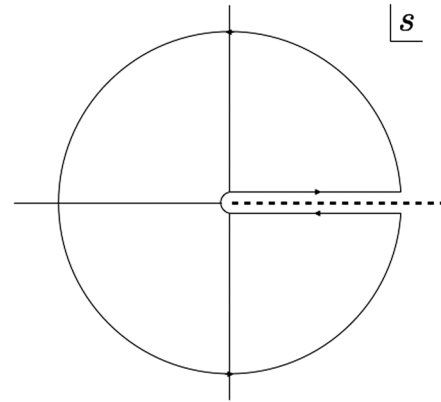


FIG. 1. Contour on the complex s plane.

$$\frac{1}{2\pi i} \oint ds \frac{\Pi(s)}{s - q^2} = \frac{1}{\pi} \int_{s_i}^{\Lambda} ds \frac{\text{Im}\Pi(s)}{s - q^2} + \frac{1}{\pi} \int_{\Lambda}^R ds \frac{\text{Im}\Pi^{\text{pert}}(s)}{s - q^2} + \frac{1}{2\pi i} \int_C ds \frac{\Pi^{\text{pert}}(s)}{s - q^2}, \quad (3)$$

where s_i in the first integral denotes the threshold for the nonvanishing spectral density $\text{Im}\Pi(s)$, the numerator in the second integrand has been replaced by the perturbative spectral density $\text{Im}\Pi^{\text{pert}}(s)$ for a sufficiently large separation scale Λ , and C in the third integral represents the large circle of radius R . The spectral density $\text{Im}\Pi(s)$ in the first integrand, involving nonperturbative dynamics from the low s region will be determined later. The perturbative function $\Pi^{\text{pert}}(s)$ in the third integral receives only the perturbative QCD contribution.

For q^2 in the deep Euclidean region, the OPE of $\Pi(q^2)$ is reliable, and we have $\Pi^{\text{pert}}(q^2)$ [1] for the left-hand side of Eq. (2),

$$\Pi^{\text{pert}}(q^2) = \frac{1}{2\pi i} \oint ds \frac{\Pi^{\text{pert}}(s)}{s - q^2} + \frac{1}{12\pi} \frac{\langle \alpha_s G^2 \rangle}{(q^2)^2} + 2 \frac{\langle m_q \bar{q}q \rangle}{(q^2)^2} + \frac{224\pi \kappa \alpha_s \langle \bar{q}q \rangle^2}{81 (q^2)^3}, \quad (4)$$

up to the dimension-six condensate, i.e., up to the power correction of $1/(q^2)^3$. In the above expression, $\langle G^2 \rangle$ is the gluon condensate, m_q is a quark mass, and the parameter $\kappa = 2-4$ [13–15] is introduced to quantify the violation in the factorization of the four-quark condensate $\langle (\bar{q}q)^2 \rangle$ into the product of $\langle \bar{q}q \rangle$. The first term on the right-hand side, collecting higher order corrections, has been expressed as the integral of the perturbative function $\Pi^{\text{pert}}(s)$ along the contour in Fig. 1.

The equality of Eq. (3) on the hadron side and Eq. (4) on the quark side leads to

$$\frac{1}{\pi} \int_{s_i}^{\Lambda} ds \frac{\text{Im}\Pi(s)}{s - q^2} = \frac{1}{\pi} \int_{s_i}^{\Lambda} ds \frac{\text{Im}\Pi^{\text{pert}}(s)}{s - q^2} + \frac{1}{12\pi} \frac{\langle \alpha_s G^2 \rangle}{(q^2)^2} + 2 \frac{\langle m_q \bar{q}q \rangle}{(q^2)^2} + \frac{224\pi \kappa \alpha_s \langle \bar{q}q \rangle^2}{81 (q^2)^3}, \quad (5)$$

where the contributions of the perturbative function $\Pi^{\text{pert}}(s)$ in the regions away from physical poles have canceled from both sides, and only the perturbative spectral density,

$$\text{Im}\Pi^{\text{pert}}(q^2) = \frac{1}{4\pi} \left(1 + \frac{\alpha_s}{\pi} \right) \equiv a\pi, \quad (6)$$

along the branch cut remains. Equation (5) is a result of the dispersion relation for the function $\Pi(q^2)$.

The next step is to parametrize the nonperturbative spectral density $\text{Im}\Pi(s)$ on the left-hand side of Eq. (5).

The translational invariance and the integration over the coordinate x in Eq. (1) gives

$$2\text{Im}\Pi_{\mu\nu}(q^2) = \sum_n \langle 0|J_{\mu}|n\rangle \langle n|J_{\nu}|0\rangle d\Phi_n (2\pi)^4 \delta(q - p_n), \quad (7)$$

for $q^2 > 0$, in which $d\Phi_n$ and p_n represent the phase space and the momentum of the intermediate state $|n\rangle$, respectively. The ground state for $|n\rangle$ is a neutral vector of the mass m_V and the polarization vector ϵ , which defines the decay constant f_V via the matrix element,

$$\langle 0|J_{\mu}|V^{\lambda}\rangle = f_V m_V \epsilon_{\mu}^{\lambda}. \quad (8)$$

The substitution of Eq. (8) into Eq. (7) yields

$$\text{Im}\Pi(q^2) = \pi f_V^2 \delta(q^2 - m_V^2) + \pi \rho^h(q^2) \theta(q^2 - s_h), \quad (9)$$

where the first term is a consequence of the narrow width approximation, and the second term describes the contribution from higher excitations with s_h being their threshold. It has been assumed that the widths of excited states become broader, so their contributions can be parametrized as a continuous spectral density function $\rho^h(q^2)$.

The key of QCD sum rules is the quark-hadron duality, which assumes that the spectral density $\rho^h(s)$ is related to the perturbative density $\text{Im}\Pi^{\text{pert}}(s)$ as s is higher than some scale $s_0 > s_h$ by

$$\rho^h(s) = \frac{1}{\pi} \text{Im}\Pi^{\text{pert}}(s) \theta(s - s_0), \quad (10)$$

referred to the local duality, or by

$$\int_{s_h}^{\Lambda} ds \frac{\rho^h(s)}{s - q^2} = \frac{1}{\pi} \int_{s_0}^{\Lambda} ds \frac{\text{Im}\Pi^{\text{pert}}(s)}{s - q^2}, \quad (11)$$

referred to the global duality. The threshold s_0 is around 1 GeV², so the duality can hardly hold at such a low scale [16,17]. Obviously, the quark-hadron duality is a major source of theoretical uncertainty, which is not easy to control.

The Borel transformation,

$$\hat{B}_M \equiv \lim_{\substack{Q^2, n \rightarrow \infty \\ Q^2/n = M^2}} \frac{1}{(n-1)!} (Q^2)^n \left(-\frac{d}{dQ^2} \right)^n, \quad (12)$$

with $Q^2 \equiv -q^2$, is then employed to suppress the continuum contribution on the hadron side, which has been related to the perturbative spectral density via the duality assumption, and to improve the OPE on the quark side. Inserting Eqs. (9) and (10) [or (11)] into Eq. (5), we derive the conventional sum rule under the Borel transformation [1],

$$f_V^2 e^{-m_V^2/M^2} = \frac{1}{\pi} \int_{s_i}^{s_0} ds \text{Im}\Pi^{\text{pert}}(s) e^{-s/M^2} + \frac{1}{12\pi} \frac{\langle \alpha_s G^2 \rangle}{M^2} + 2 \frac{\langle m_q \bar{q}q \rangle}{M^2} - \frac{112\pi \kappa \alpha_s \langle \bar{q}q \rangle^2}{81 M^4}. \quad (13)$$

It is seen that the suppression on the higher power corrections with the typical $M \sim O(1)$ GeV and by the additional factors $1/(k-1)!$ for the $1/(q^2)^k$ term, $k \leq 3$, is not effective actually. The prescription for a sum rule calculation is to tune the threshold s_0 in the above formula, such that the value of f_V is stable against the variation of the Borel mass M in a maximal window of M . This prescription introduces theoretical uncertainty, especially when the sum rule window does not exist [2].

An alternative interpretation for the equality of the hadron and quark sides in Eq. (5) is that there exist multiple solutions to Eq. (2): the right-hand side of Eq. (3), which contains the nonperturbative spectral density $\text{Im}\Pi(s)$ in the first term, can be regarded as a nonperturbative solution to Eq. (2), while the right-hand side of Eq. (4) can be regarded as a perturbative solution. Motivated by the above viewpoint, we propose to handle QCD sum rules as an inverse problem, for which multiple solutions exist naturally. First, the spectral density is written as the superposition of the pole and continuum contributions,

$$\text{Im}\Pi(q^2) = \pi f_V^2 \delta(q^2 - m_V^2) + \pi \rho^h(q^2), \quad (14)$$

where the threshold s_h in Eq. (9), introduced in conventional sum rules to characterize the continuum region, does not appear. As mentioned before, excited states tend to have broader widths, and the transition from the resonance to continuum region should be smooth. Hence, the second term in Eq. (14) behaves more like a ramp function [18] in general, taking a value as $q^2 > s_i$, instead of like a step function. The unknown function $\pi \rho^h(q^2)$ can be approximated by the perturbative spectral density $\text{Im}\Pi^{\text{pert}}(q^2)$ reliably as q^2 is great than some large separation scale Λ as shown in Eq. (3). Strictly speaking, this approximation is also based on the local quark-hadron duality, but it is not the concerned duality assumption in conventional QCD sum rules around the threshold $s_0 \approx 1 \text{ GeV}^2$, and the duality violation above the large Λ is expected to be minor.

Inserting Eq. (14) into the left-hand side of Eq. (5), we write

$$\begin{aligned} \frac{f_V^2}{m_V^2 - q^2} + \int_0^\Lambda ds \frac{\rho^h(s)}{s - q^2} &= \omega(q^2), \\ \omega(q^2) &= a \ln \frac{q^2 - \Lambda}{q^2} + \frac{1}{12\pi} \frac{\langle \alpha_s G^2 \rangle}{(q^2)^2} + 2 \frac{\langle m_q \bar{q}q \rangle}{(q^2)^2} \\ &\quad + \frac{224\pi \kappa \alpha_s \langle \bar{q}q \rangle^2}{81 (q^2)^3}, \end{aligned} \quad (15)$$

in which the threshold $s_i = 4m_\pi^2$ with the pion mass m_π has been set to zero, and the OPE input $\omega(q^2)$, equal to the right-hand side of Eq. (5), is calculable as a standard OPE. The sum rule is then turned into an inverse problem, where the unknowns m_V , f_V and $\rho^h(s)$ are solved with the OPE input $\omega(q^2)$. The suppression on the uncertain continuum contribution, which will be solved directly, is not necessary. The suppression on the higher power corrections can be easily achieved by considering the input $\omega(q^2)$ at large $|q^2|$. Applying the Borel transformation to Eq. (15), we get

$$\begin{aligned} \frac{f_V^2}{M^2} e^{-m_V^2/M^2} + \frac{1}{M^2} \int_0^\Lambda ds \rho^h(s) e^{-s/M^2} &= \hat{\omega}(M^2), \\ \hat{\omega}(M^2) &\equiv \hat{B}_M \omega(q^2) = a(1 - e^{-\Lambda/M^2}) \\ &\quad + \frac{1}{12\pi} \frac{\langle \alpha_s G^2 \rangle}{(M^2)^2} + 2 \frac{\langle m_q \bar{q}q \rangle}{(M^2)^2} - \frac{112\pi \kappa \alpha_s \langle \bar{q}q \rangle^2}{81 (M^2)^3}. \end{aligned} \quad (16)$$

As demonstrated in the next section, both versions, Eqs. (15) and (16), give similar solutions to the unknowns. Therefore, we postulate that the Borel transformation is not crucial for the present formalism.

Note that an inverse problem is usually ill-posed, and the ordinary discretization method to solve a Fredholm integral equation does not work. The best fit method proposed in [19] may be the most transparent way to reveal the existence of multiple solutions in this case. To facilitate the numerical analysis, we expand the spectral density function $\rho^h(y) \equiv \rho^h(s = y\Lambda)$ in Eq. (15) in a series of Legendre polynomials,

$$\begin{aligned} \rho^h(y) &= b_0 P_0(2y - 1) + b_1 P_1(2y - 1) + b_2 P_2(2y - 1) \\ &\quad + b_3 P_3(2y - 1) + \dots, \end{aligned} \quad (17)$$

with

$$\begin{aligned} P_0(y) &= 1, & P_1(y) &= y, & P_2(y) &= \frac{1}{2}(3y^2 - 1), \\ P_3(y) &= \frac{1}{2}(5y^3 - 3y). \end{aligned} \quad (18)$$

Other bases of orthogonal functions, such as the trigonometric functions, can serve the purpose equally well. The boundary conditions $\rho^h(0) = 0$ and $\rho^h(1) = a$ (equal to the perturbative density at $s = \Lambda$) impose the constraints,

$$b_2 = \frac{a}{2} - b_0, \quad b_3 = \frac{a}{2} - b_1. \quad (19)$$

It will be verified that the expansion up to $P_3(y)$, with the converging coefficients b_i , is sufficient. We will solve Eq. (15) by tuning Λ , m_V , f_V , b_0 , and b_1 to minimize the difference between its two sides.

III. APPLICATIONS

In this section, we extract the observables associated with the series of ρ resonances from our formalism. It is notoriously difficult to solve a Fredholm integral equation like Eq. (15). We have found that the best fit method may be the most transparent way to probe multiple solutions of a Fredholm equation, which has been applied to the explanation of the D meson mixing parameters [19] and the determination of the hadronic vacuum polarization contribution to the muon anomalous magnetic moment [20]. The following OPE parameters [21,22] and the strong coupling evaluated at the scale of 1 GeV are adopted,

$$\begin{aligned} \Lambda_{\text{QCD}} &= 0.353 \text{ GeV}, & \langle m_q \bar{q} q \rangle &= 0.007 \times (-0.246)^3 \text{ GeV}^4, \\ \langle \alpha_s G G \rangle &= 0.07 \text{ GeV}^4, \\ \alpha_s \langle \bar{q} q \rangle^2 &= 1.49 \times 10^{-4} \text{ GeV}^6, & \alpha_s &= 0.5. \end{aligned} \quad (20)$$

We consider the input $\omega(q^2)$ from an appropriate range of q^2 in the Euclidean region, in which 20 points q_i^2 are selected, and then search for the set of parameters Λ , m_V , f_V , b_0 , and b_1 that minimizes the residual sum of square (RSS),

$$\sum_{i=1}^{20} \left| \frac{f_V^2}{m_V^2 - q_i^2} + \int_0^\Lambda ds \frac{\rho^h(s)}{s - q_i^2} - \omega(q_i^2) \right|^2. \quad (21)$$

Such a set of parameters approximates a solution of the Fredholm equation (15). A similar RSS can be defined for the sum rule in Eq. (16) under the Borel transformation, for which the input $\hat{\omega}(M^2)$ is selected from an appropriate range of $M^2 > 0$. We have tested the number of input points from 20 to 500 and confirmed that solutions do not alter.

A. Ground state

The scanning over all the free parameters reveals the minima of the RSS defined in Eq. (21). We present the distributions of the RSS minima on the $\Lambda - m_V$ planes in Fig. 2 and on the $\Lambda - f_V$ planes in Fig. 3, where each array contains three columns of plots for $\kappa = 2, 3$, and 4, and three rows for the OPE inputs from the ranges $(-100 \text{ GeV}^2, -1 \text{ GeV}^2)$ in q^2 , $(-100 \text{ GeV}^2, -10 \text{ GeV}^2)$ in q^2 , and $(1 \text{ GeV}^2, 100 \text{ GeV}^2)$ in M^2 . The reason why the input point is extended to $q^2 = -100 \text{ GeV}^2$ ($M^2 = 100 \text{ GeV}^2$) is that we intend to find a solution to Eq. (15) [Eq. (16)] in a large range of q^2 (M^2). Nontrivial landscapes of the RSS minima are observed, which imply the resonance masses m_V and the decay constants f_V preferred by the sum rule in Eqs. (15) or (16). A point on a curve of deep color, having RSS about 10^{-14} (10^{-18}) relative to 10^{-8} (10^{-10}) from outside the curve in the first and third (second) rows, represents an approximate solution to the sum rules. A solution in the segment of the curve with deeper color is closer to the exact solution, and the finite

length of this segment hints the existence of multiple solutions. A value of Λ labels the scale, below which the nonperturbative continuum contribution starts to deviate from the OPE input, so its variation affects the solutions of m_V and f_V . This explains the dependence of the preferred m_V and f_V on Λ , described by the minimum distributions.

It is expected that the power corrections would be enhanced with the input range $(-100 \text{ GeV}^2, -1 \text{ GeV}^2)$ in q^2 compared to $(-100 \text{ GeV}^2, -10 \text{ GeV}^2)$ because the former covers the low Q^2 region. The enhancement is reflected by the sensitivity of the RSS minimum distributions to the variation of κ in the first row of plots stronger than in the second row. The dependence of the minimum distributions on κ is also more obvious in the third row with the input from low M^2 . Note that the dimension-six four-quark condensate correction becomes comparable to the dimension-four gluon condensate correction, both being of order of 10^{-3} , at Q^2 and M^2 as low as $O(1) \text{ GeV}^2$. The minimum distributions obtained from Eq. (16) are similar to those from Eq. (15): the minimum locations on the planes in the third rows are somewhat between those in the first and second rows of Figs. 2 and 3. It is understood, since the coefficient of the dimension-six condensate in Eq. (16) is half of that in Eq. (15), and this reduction can be mimicked by selecting the input from a larger Q^2 region for Eq. (15). The above similarity supports the equivalence of Eqs. (15) and (16), and our postulation that the Borel transformation is not needed, once sum rules are treated as an inverse problem. We will focus only on Eq. (15) for numerical analyses from now on. As to the input range, we pick up the one, where the perturbative term is relatively more important than the condensate corrections, and the OPE is sufficiently convergent, namely $(-100 \text{ GeV}^2, -10 \text{ GeV}^2)$ in q^2 . It has been checked that the input range $(-100 \text{ GeV}^2, -5 \text{ GeV}^2)$ in q^2 leads to the minimum distributions on the $\Lambda - m_V$ and $\Lambda - f_V$ planes almost identical to the middle rows of Figs. 2 and 3, respectively.

It is interesting to see that two branches of minimum distributions appear on the $\Lambda - m_V$ planes with a gap between them, and the lower ones, being roughly flat (independent of Λ), are located around $m_V \approx 0.8 \text{ GeV}$, which is close to the $\rho(770)$ meson mass $m_{\rho(770)}$. It has been claimed, based on a stable analytic extrapolation [23], that the present perturbative amplitude in the deep Euclidean region produces a prominent bump structure in the resonance region. Here, we have explicitly shown that the ground state $\rho(770)$ is predicted by our formalism. The depth of color in the second row of Fig. 2 indicates that global minima along the lower distributions appear in the range $2 \text{ GeV}^2 < \Lambda < 4 \text{ GeV}^2$. We point out that the minimum distribution in the central plot of Fig. 2 is flat, up to $\Lambda = 6 \text{ GeV}^2$, a behavior which can be regarded as kind of stability. The predicted $\rho(770)$ meson mass read off

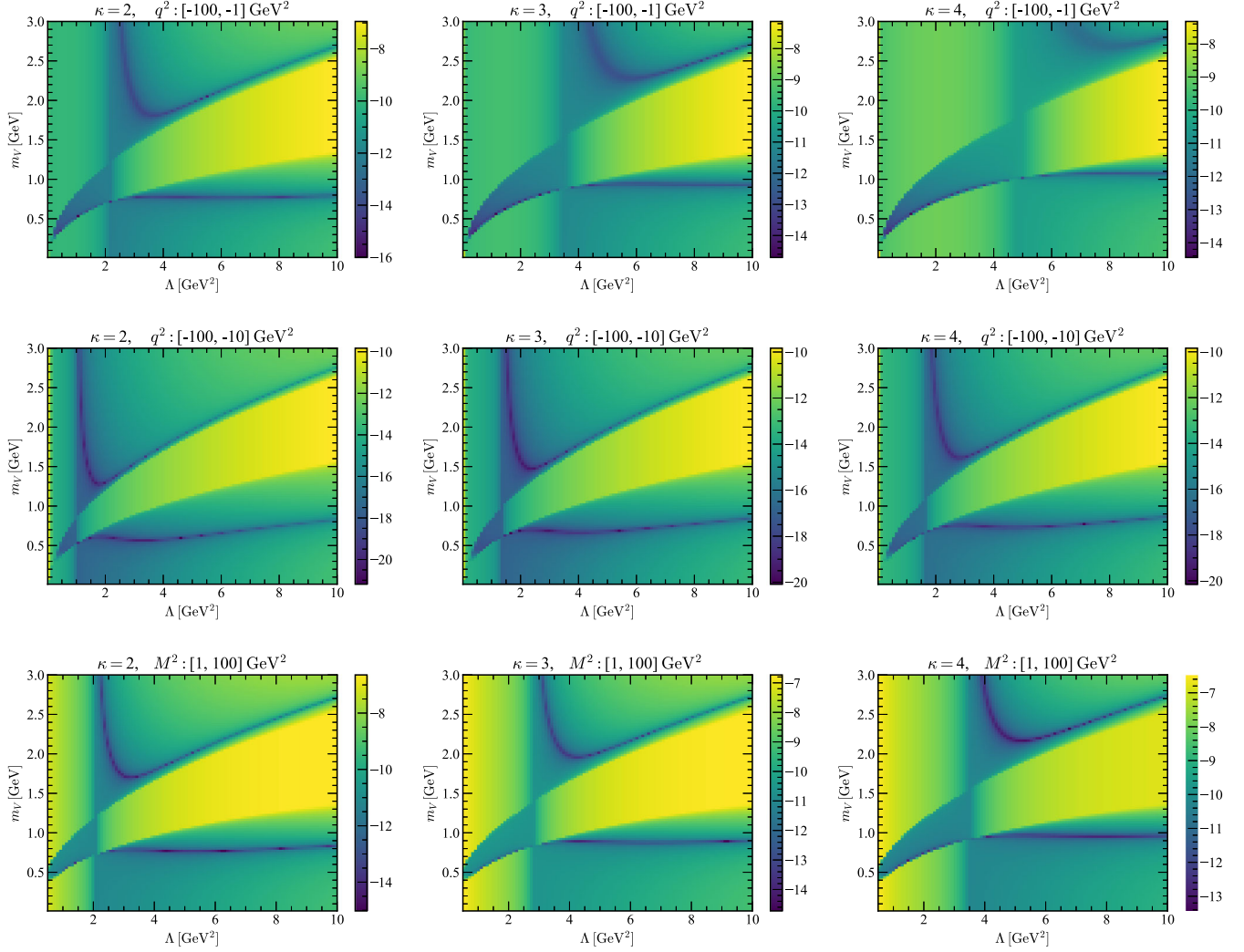


FIG. 2. Minimum distributions of RSS defined in Eq. (21) on the $\Lambda - m_V$ planes for $\kappa = 2, 3$, and 4 with the input ranges $(-100 \text{ GeV}^2, -1 \text{ GeV}^2)$ in q^2 , $(-100 \text{ GeV}^2, -10 \text{ GeV}^2)$ in q^2 , and $(1 \text{ GeV}^2, 100 \text{ GeV}^2)$ in M^2 .

from the above range is not sensitive to the parameter κ : it increases by about 10% when κ changes from 3 to 4, consistent with what was observed in [21]. The upper minimum distributions in the $\Lambda - m_V$ plots imply that the single pole parametrization in Eq. (14) allows a larger m_V to be a solution to Eq. (15). Note that Eq. (14) simply parametrizes the contribution from a resonance and a continuum, so the resonance does not correspond to the $\rho(770)$ meson *a priori*. It is likely that the contribution from an excited state and a continuum also obeys the Fredholm equation and serves as one of the allowed multiple solutions. Therefore, we conjecture that the upper distributions are associated with excited states, whose significance will be explored in the next subsection.

There is only a single RSS minimum distribution on each $\Lambda - f_V$ plane in Fig. 3. It is possible, if the ground state and the first excited state had similar decay constants. The plots in the second row imply a weaker dependence of the minimum distributions on Λ than in the first and third rows.

These minimum distributions are located around $f_V \approx 0.2 \text{ GeV}$, close to the decay constant of the $\rho(770)$ meson. A larger κ value, i.e., a larger four-quark condensate tends to increase f_V . In particular, the second row of Fig. 3 reveals global minima in the range $2 \text{ GeV}^2 < \Lambda < 4 \text{ GeV}^2$, the same as in the second row of Fig. 2. This consistency hints that the best solutions to the sum rule in Eq. (15) can accommodate the physical values of the $\rho(770)$ meson mass and decay constant simultaneously.

We first fix the factorization violation parameter κ associated with the four-quark condensate using the $\rho(770)$ meson mass $m_{\rho(770)} \approx 0.78 \text{ GeV}$ and adopt this κ value for further analyses. It is straightforward to find that the $\rho(770)$ meson mass can be produced with $\kappa = 3.2$, a value also preferred by [15], along the lower minimum distribution in a wide range $2 \text{ GeV}^2 < \Lambda < 6 \text{ GeV}^2$ as shown in Fig. 4(a). Since we have ensured that both the best fitted m_V and f_V occur roughly in the same range of Λ , we determine f_V in a less ambiguous way by setting m_V to

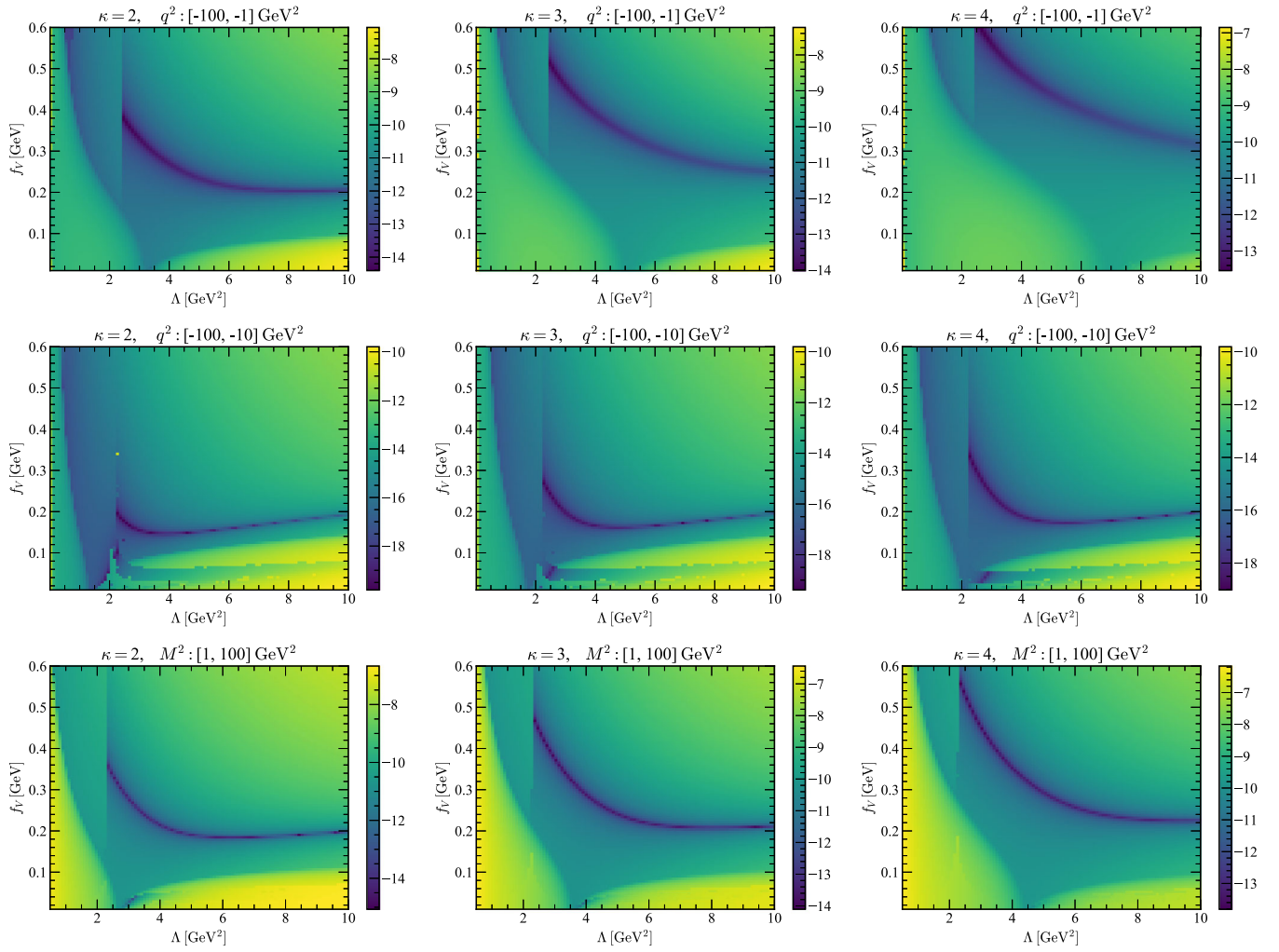


FIG. 3. Minimum distributions of RSS defined in Eq. (21) on the $\Lambda - f_V$ planes for $\kappa = 2, 3$, and 4 with the input ranges $(-100 \text{ GeV}^2, -1 \text{ GeV}^2)$ in q^2 , $(-100 \text{ GeV}^2, -10 \text{ GeV}^2)$ in q^2 , and $(1 \text{ GeV}^2, 100 \text{ GeV}^2)$ in M^2 .

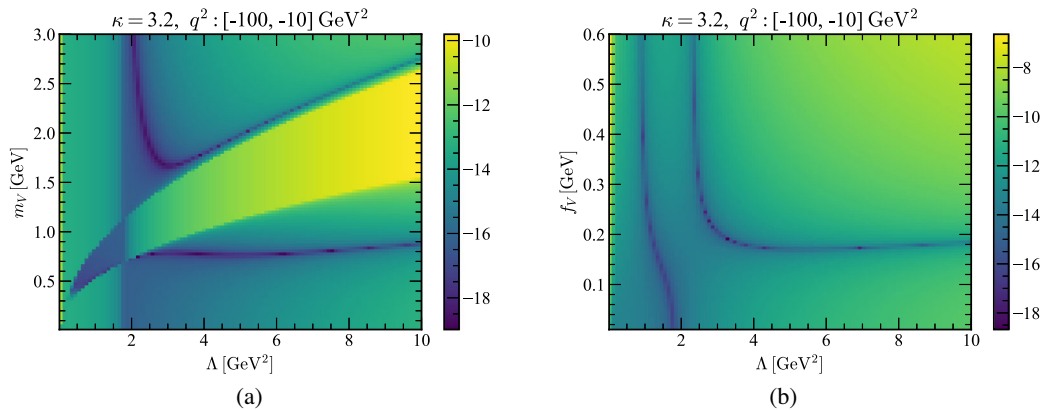


FIG. 4. Minimum distributions of RSS (a) on the $\Lambda - m_V$ plane for $\kappa = 3.2$ with the input range $(-100 \text{ GeV}^2, -10 \text{ GeV}^2)$ in q^2 , and (b) on the $\Lambda - f_V$ with m_V being further set to $m_{\rho(770)} \approx 0.78 \text{ GeV}$.

$m_{\rho(770)} \approx 0.78$ GeV to avoid possible influence from excited states. The resultant $\Lambda - f_V$ plot from Eq. (15) with the input range $(-100 \text{ GeV}^2, -10 \text{ GeV}^2)$ in q^2 is displayed in Fig. 4(b). For consistency, we search for the global minimum in the range $2 \text{ GeV}^2 < \Lambda < 6 \text{ GeV}^2$ and find that the one located at $\Lambda = 2.8 \text{ GeV}^2$ on the L-shape distribution gives the decay constant $f_{\rho(770)} = 0.22$ GeV. The separation scale $\Lambda = 2.8 \text{ GeV}^2$ is supposed to be large enough for justifying the replacement of $\text{Im}\Pi(s)$ by $\text{Im}\Pi^{\text{pert}}(s)$ in the second term on the right-hand side of Eq. (3). The above results of $m_{\rho(770)}$ and $f_{\rho(770)}$ agree with those in [24], from the lattice calculation [25], from the Bethe-Salpeter equation [26–28], and from the light-front quark model [29].

To test the sensitivity of our results to the OPE uncertainties, we vary the perturbative piece and the quark condensate $\langle \bar{q}q \rangle$ by $\pm 30\%$ separately. It is observed that our results are less sensitive to the variation of the former. Since the quark condensate and the gluon condensate appear at the same power of $1/(q^2)^2$, the 30% variation can include and mimic that from the gluon condensate. It is understood that the $\langle \bar{q}q \rangle^2$ term at the power $1/(q^2)^3$ also varies accordingly. We find that the $\rho(770)$ meson mass, extracted from the single-pole parametrization in Eq. (15), differs by only about $\pm 15\%$. It implies that our results in the present setup are stable, as the OPE uncertainties are taken into account.

We also read off the coefficients in the expansion of the spectral density function $\rho^h(q^2)$ in terms of the Legendre polynomials, which correspond to the selected global minimum located at $\Lambda = 2.8 \text{ GeV}^2$ in Fig. 4(b),

$$\begin{aligned}
 b_0 &= 0.0126, & b_1 &= 0.0276, \\
 b_2 &= 0.0022, & b_3 &= -0.0128.
 \end{aligned} \quad (22)$$

As two more Legendre polynomials P_4 and P_5 are included in the expansion, the global minimum shifts to $\Lambda = 3.1 \text{ GeV}^2$

with the corresponding decay constant $f_{\rho(770)} = 0.23$ GeV, and we have

$$\begin{aligned}
 b_0 &= 0.0120, & b_1 &= 0.0308, & b_2 &= -0.0040, \\
 b_3 &= -0.0202, & b_4 &= 0.0068, & b_5 &= 0.0042.
 \end{aligned} \quad (23)$$

The stability of the coefficients b_0, \dots, b_3 and the smallness of b_4 and b_5 verify that the expansion up to the polynomial P_3 is enough.

The behavior of the spectral density function $\rho^h(q^2)$ in q^2 for Eq. (22) is depicted in Fig. 5(a), which differs dramatically from the step function in Eq. (10) based on the local quark-hadron duality. Note that the slope of the solved $\rho^h(q^2)$ is discontinuous at $q^2 = \Lambda = 2.8 \text{ GeV}^2$, where it transits to the perturbative spectra density function because we have not yet imposed the continuity constraint to the slope. The exact spectral density should approach to the perturbative one at a sufficiently large Λ , such that a solution becomes less sensitive to the choice of the separation scale Λ . This explains the flatness of the minimum distribution for $\Lambda > 4 \text{ GeV}^2$ in Fig. 4(b). The function $\rho^h(q^2)$ is slightly negative at q^2 , where the pole is located. This negative contribution is expected to be compensated by that from the resonance, when its finite width is taken into account. We mention that the minimum distribution on the $\Lambda - f_V$ plane in Fig. 4(b) becomes nearly vertical at $\Lambda \approx 2.3 \text{ GeV}^2$, corresponding to solutions with large f_V . It is easy to find that the corresponding function $\rho^h(q^2)$ is significantly negative at the $\rho(770)$ pole, so f_V must be large to compensate this negative contribution.

We compare the q^2 dependencies of the left-hand side from the best fit solution and of the right-hand side of Eq. (15) by showing their difference in Fig. 5(b). For the purpose of comparison, we display a solution on the minimum distribution located at $\Lambda = 10 \text{ GeV}^2$ in Fig. 4(b) with the corresponding decay constant $f_V = 0.18$ GeV, which is far away from the global minimum. It is obvious that the

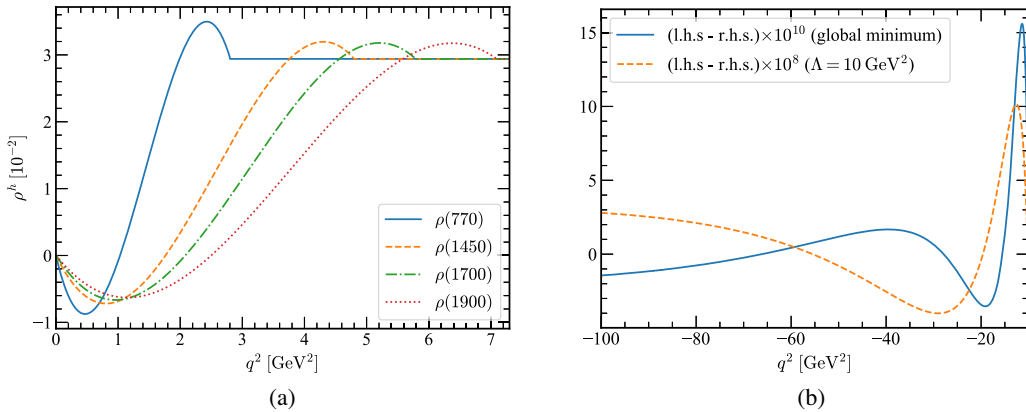


FIG. 5. (a) Behavior of the spectral density function $\rho^h(q^2)$ in q^2 , and (b) difference between the two sides of Eq. (15) for the best fit solution in Fig. 4(b), and a solution on the minimum distribution located at $\Lambda = 10 \text{ GeV}^2$.

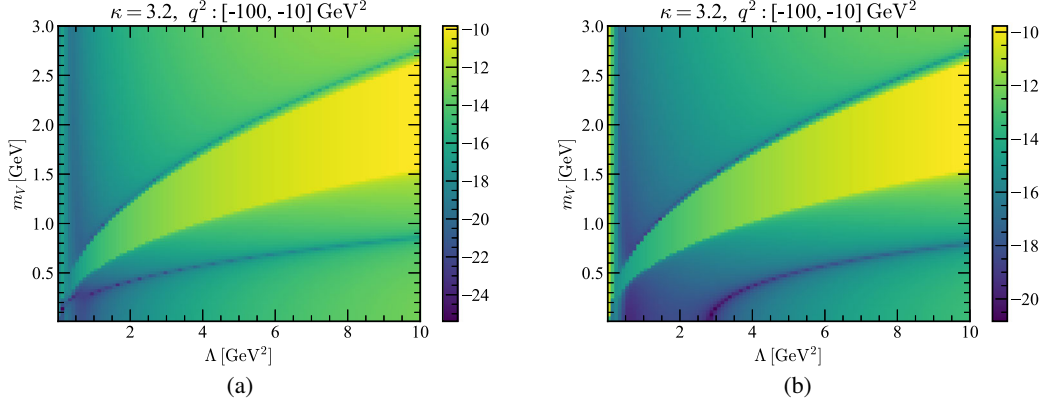


FIG. 6. Minimum distributions of RSS on the $\Lambda - m_V$ planes for $\kappa = 3.2$ with the input of (a) the perturbative piece only, and (b) without the $1/(q^2)^3$ power correction from the range $(-100 \text{ GeV}^2, -10 \text{ GeV}^2)$ in q^2 .

two sides of Eq. (15) match each other well in the former case and that the difference between the two sides is about 100 times larger in the latter case.

Next, we investigate how each term in the OPE input influences the emergence of the ρ resonances in Fig. 2. The RSS minimum distributions on the $\Lambda - m_V$ plane for the two cases, with only the perturbative piece and without the $1/(q^2)^3$ power correction, are presented in Figs. 6(a) and 6(b), respectively. It is seen that both the minimum distributions grow with Λ in the former without a stable region. It implies that the perturbative piece alone does not induce a bound state. When the $1/(q^2)^2$ terms, i.e., the gluon and two-quark condensates, are turned on, the lower minimum distribution in Fig. 6(b) shifts toward the larger Λ region but still does not exhibit a stable value of m_V . The upper minimum distribution remains as dim as in Fig. 6(a). When all the terms on the right-hand sides of Eq. (15) are present, the stable ground state mass appears, and the upper minimum distribution also gets enhanced as shown in Fig. 4. The observation is that all the terms in the OPE work together to generate the ρ resonance, and the four-quark condensate is more crucial for its emergence.

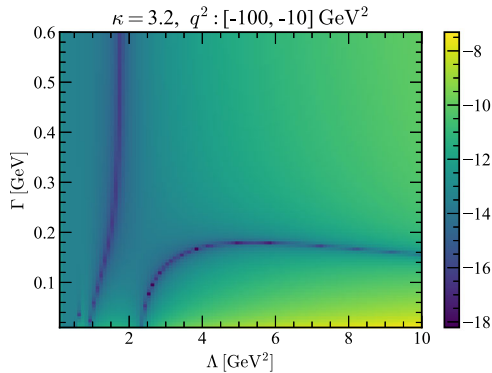


FIG. 7. Minimum distribution of RSS on the $\Lambda - \Gamma$ plane for $\kappa = 3.2$ with the input from the range $(-100 \text{ GeV}^2, -10 \text{ GeV}^2)$ in q^2 .

Below we extract the ρ meson decay width from our formalism by inserting the $\pi^+\pi^-$ state and other multi-hadron states into the correlator in Eq. (1), among which the matrix element $\langle 0|J_\mu|\pi^+\pi^- \rangle$ defines the time-like pion form factor. The ρ resonance contributes to the spectral density dominantly, which is parametrized as [21,30]

$$\text{Im}\Pi(q^2) = \frac{1}{24\pi} \frac{m_V^4 + m_V^2\Gamma^2}{(q^2 - m_V^2)^2 + m_V^2\Gamma^2} + \pi\rho^h(q^2), \quad (24)$$

with the width Γ . The first term in the above expression corresponds to the timelike pion form factor, which describes the decay of a ρ meson, produced by the current J_μ , into a pion pair. No three pion states are involved here, which arise from an ω resonance suppressed by the isospin-1 current. The boundary condition $\rho^h(q^2 = \Lambda) = a$ ought to be modified into $\text{Im}\Pi(q^2 = \Lambda) = a\pi$ due to the finite distribution of the form factor in q^2 . We set $m_V = m_{\rho(770)}$ and analyze the minimum distribution on the $\Lambda - \Gamma$ plane, which is exhibited in Fig. 7. Other parametrizations for the timelike pion form factor, such as the Breit-Wigner one in [31], have been tested, and similar minimum distributions are obtained. It is noticed that the global minimum located at $\Lambda = 4.3 \text{ GeV}^2$ gives $\Gamma = 0.17 \text{ GeV}$, close to the value in [24]. We mention that it is difficult to reproduce the width of the $\rho(770)$ meson with any reasonable precision in the Bayesian approach [4] because of the insufficient sensitivity of the detailed $\rho(770)$ peak form to the OPE input.

B. Excited states

The upper minimum distributions on the $\Lambda - m_V$ planes in Fig. 2, with a gap above the lower ones, hint strongly the existence of other resonances, though a single pole parametrization for the spectral density was adopted in Eq. (14). Combining the implication of the $\Lambda - f_V$ plots in Fig. 3, we speculate that an excited ρ state with the decay constant around 0.2 GeV can also satisfy the sum rule in Eq. (15). Compared to the lower minimum distributions, referred to

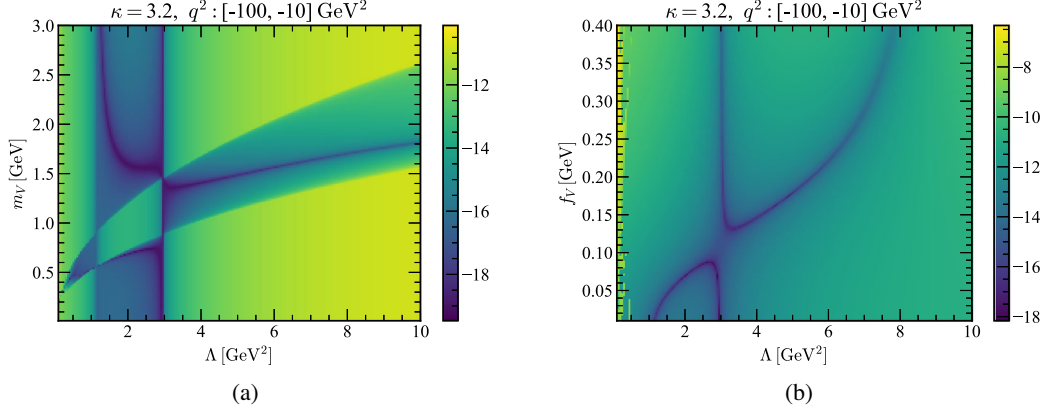


FIG. 8. Minimum distributions of RSS (a) on the $\Lambda - m_V$ plane for the double pole parametrization with $\kappa = 3.2$ and the input range $(-100 \text{ GeV}^2, -10 \text{ GeV}^2)$ in q^2 , and (b) on the $\Lambda - f_V$ plane with m_V being further set to $m_{\rho(1450)} = 1.46 \text{ GeV}$.

the ground state $\rho(770)$, the minimum distributions associated with excited states exhibit more significant sensitivity to the variation of the separation scale Λ . This is understandable because more excited states, which are denser in the mass spectrum, will be covered as Λ increases, such that a single pole parametrization becomes less proper. To study properties of an excited state, we modify the spectral density in Eq. (14) into

$$\text{Im}\Pi(q^2) = \pi f_{\rho(770)}^2 \delta(q^2 - m_{\rho(770)}^2) + \pi f_V^2 \delta(q^2 - m_V^2) + \pi \rho^h(q^2), \quad (25)$$

where the ground state mass and decay constant have been fixed to $m_{\rho(770)} = 0.78 \text{ GeV}$ and $f_{\rho(770)} = 0.22 \text{ GeV}$ determined in the previous subsection. The first excited state has been moved out of the continuum and treated as the second isolated resonance in the above parametrization. Certainly, the RSS definition in Eq. (21) is also modified accordingly with two resonance terms being included.

We observe the RSS minimum distribution on the $\Lambda - m_V$ plane with the OPE input range $(-100 \text{ GeV}^2, -10 \text{ GeV}^2)$ in q^2 and $\kappa = 3.2$ in Fig. 8(a). Given the double pole parametrization in Eq. (25), the minimum distribution indeed becomes less Λ dependent at large Λ , compared to the upper minimum distribution in Fig. 4(a). In particular, global minima in the range $\Lambda \approx 3\text{--}5 \text{ GeV}^2$ imply the preferred values of m_V close to the $\rho(1450)$ meson mass $m_{\rho(1450)} \approx 1.46 \text{ GeV}$. That is, we find the indication for the existence of the first excited ρ state in our formalism. We mention that the extraction of higher resonance properties is more sensitive to the variation of the OPE input, compared to the extraction of the ground state properties: the 30% variation of the quark condensate $\langle \bar{q}q \rangle$ causes more than 20% difference in the determination of the $\rho(1450)$ meson mass. A seeming U-shape minimum distribution attaches to the tilted one without a gap, a layout quite different from Fig. 4(a). Note that there may

exist another state $\rho(1570)$ with a similar mass, which has been speculated to be due to an Okubo-Zweig-Iizuka-suppressed decay mode of $\rho(1700)$ [24]. It is not clear whether the gapless minimum distributions are related to these two nearby states $\rho(1450)$ and $\rho(1570)$. A more precise OPE input may help clarify this issue.

Since extremely low values of RSS have been observed in Fig. 4 for the one resonance study, the sum rule is quite stable, and the OPE input could be described well by one resonance; it is a concern whether we have overfit the OPE input using the double-pole parametrization in Eq. (25). To clarify this concern and whether new information on higher resonances can be extracted, we treat both the masses m_{V_1} and m_{V_2} , and both the decay constants f_{V_1} and f_{V_2} as free parameters in a double-pole parametrization, and then scan the $m_{V_1} - m_{V_2}$ plane around $\Lambda \approx 2 \text{ GeV}^2$ with $\kappa = 3.2$ to search for the RSS minimum distribution. It is intriguing to see in Fig. 9 that the region with $m_{V_1} \approx m_{V_2}$, namely, a single-state solution is not favored compared to the two-state solution. With more free parameters, the uncertainty in

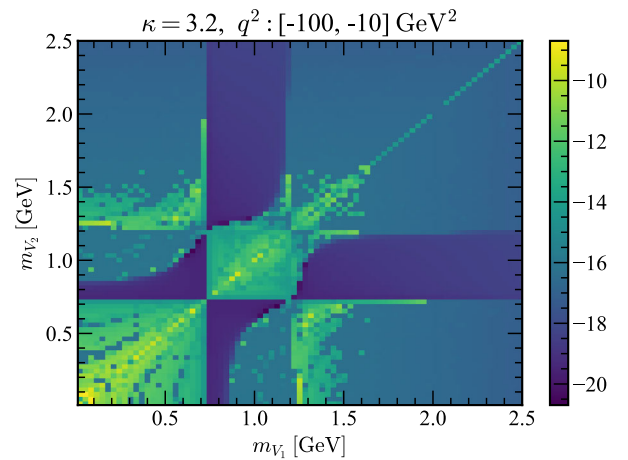


FIG. 9. RSS minimum distribution on the $m_{V_1} - m_{V_2}$ plane in the double-pole parametrization around $\Lambda \approx 2 \text{ GeV}^2$ with $\kappa = 3.2$.

the fit is larger, as indicated by the wide dark bands, and the numerical fluctuation is more violent. It is the reason why we performed the fit and determined the mass one resonance after another in order to control the precision. Nevertheless, global minima are still identified in Fig. 9, which hint at a state with a lower mass of about 0.8 GeV and another state with a higher mass of about 1.3 GeV. Therefore, nontrivial new information on higher resonances can indeed be extracted from the OPE input through the sum rules.

We then choose m_V in Eq. (25) as $m_{\rho(1450)} = 1.46$ GeV, namely, fix the considered excited state to be $\rho(1450)$ and find the minimum distribution on the $\Lambda - f_V$ plane in Fig. 8(b). We discard the distribution in the low Λ region, since the separation scale should be higher than $m_{\rho(1450)}^2$ in the search for a physical solution of the double pole parametrization. The preferred decay constant $f_{\rho(1450)} = 0.19$ GeV is read off from the global minimum located at $\Lambda = 4.8$ GeV². This value of $f_{\rho(1450)}$ leads to the ratio of the two τ decay widths,

$$\frac{\Gamma(\tau \rightarrow \rho(1450)\nu_\tau)}{\Gamma(\tau \rightarrow \rho(770)\nu_\tau)} = \frac{(m_\tau^2 - m_{\rho(1450)}^2)f_{\rho(1450)}^2}{(m_\tau^2 - m_{\rho(770)}^2)f_{\rho(770)}^2} \approx 0.3, \quad (26)$$

for the masses $m_\tau = 1.777$ GeV, $m_{\rho(770)} = 0.775$ GeV, and $m_{\rho(1450)} = 1.465$ GeV, and the decay constant $f_{\rho(770)} = 0.22$ GeV. The above ratio, being larger than the estimate 0.1 in the extended Nambu-Jona-Lasinio model [32], can be confronted with future data.

We point out that the continuum contribution to the spectral density differs from the one described by Eq. (22) because the first excited state $\rho(1450)$ has been moved out of the continuum. The coefficients of the Legendre polynomials corresponding to the global minimum in Fig. 8(b) are

$$\begin{aligned} b_0 &= 0.0104, & b_1 &= 0.0248, \\ b_2 &= 0.0033, & b_3 &= -0.0101, \end{aligned} \quad (27)$$

so the expansion of the spectral density function up to the P_3 term is still enough. The behavior of the spectral density function $\rho^h(q^2)$ in q^2 is displayed in Fig. 5(a), which differs from the step function in Eq. (10) and from the one associated with the single pole solution. It is natural that $\rho^h(q^2)$ becomes sizable at higher q^2 , when more resonances are moved out of the continuum. Without the duality assumption on the hadron side, there is more freedom to adjust the continuum contribution according to considered resonances.

The strategy to extract the observables associated with the next excited state is clear now in our formalism. The study of higher excited states is expected to be more difficult since they become denser in the mass spectrum. Motivated by the appearance of the additional U-shape minimum distribution on the $\Lambda - m_V$ plane in Fig. 10(a), we repeat the procedure. To examine whether there exist higher excited states, we further modify the spectral density into

$$\begin{aligned} \text{Im}\Pi(q^2) &= \pi f_{\rho(770)}^2 \delta(q^2 - m_{\rho(770)}^2) \\ &\quad + \pi f_{\rho(1450)}^2 \delta(q^2 - m_{\rho(1450)}^2) \\ &\quad + \pi f_V^2 \delta(q^2 - m_V^2) + \pi \rho^h(q^2), \end{aligned} \quad (28)$$

where the mass and the decay constant of the $\rho(1450)$ meson have been set to $m_{\rho(1450)} = 1.46$ GeV and $f_{\rho(1450)} = 0.19$ GeV derived above, respectively. The RSS minimum distribution on the $\Lambda - m_V$ plane with the OPE input range (-100 GeV², -10 GeV²) in q^2 and $\kappa = 3.2$ is presented in Fig. 10(a). The U-shape minimum distribution appears again, but with a gap above the slightly tilted one. It is easy to find the global minima located on the tilted minimum distribution around $\Lambda \sim 5$ GeV², which correspond to

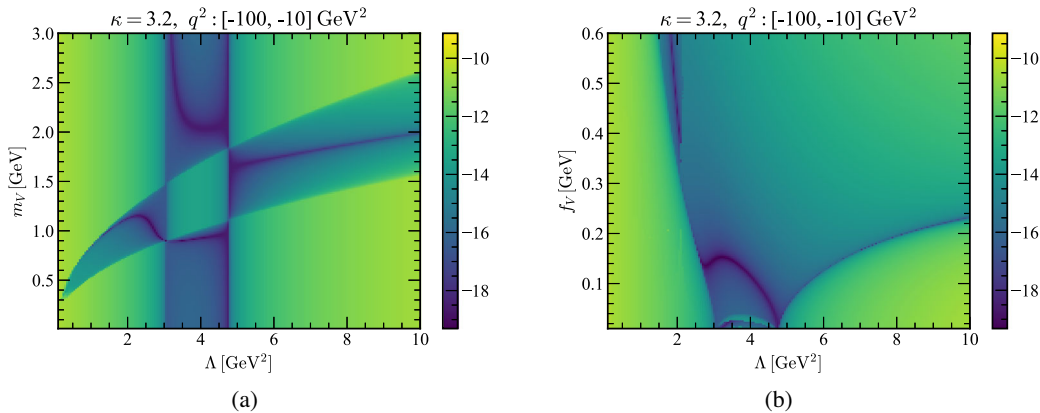


FIG. 10. Minimum distributions of RSS (a) on the $\Lambda - m_V$ plane for the triple pole parametrization with $\kappa = 3.2$ and the input range (-100 GeV², -10 GeV²) in q^2 , and (b) on the $\Lambda - f_V$ plane with m_V being further set to $m_{\rho(1700)} = 1.7$ GeV.

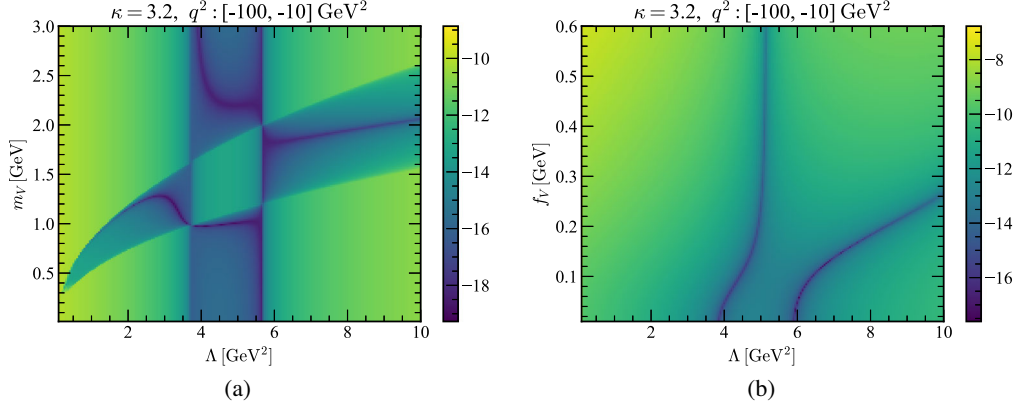


FIG. 11. Minimum distributions of RSS (a) on the $\Lambda - m_V$ plane for the quadruple pole parametrization with $\kappa = 3.2$ and the input range $(-100 \text{ GeV}^2, -10 \text{ GeV}^2)$ in q^2 , and (b) on the $\Lambda - f_V$ plane with m_V being further set to $m_{\rho(1900)} = 1.9 \text{ GeV}$.

$m_V \approx 1.7 \text{ GeV}$, exactly the $\rho(1700)$ meson mass [24]. That is, the second excited ρ state also emerges in our formalism.

We then search the minimum distribution on the $\Lambda - f_V$ plane with m_V being set to the value of $m_{\rho(1700)} = 1.7 \text{ GeV}$, namely, with the considered excited state being fixed to $\rho(1700)$. The minimum distribution, displayed in Fig. 10(b), also reveals a nontrivial structure. We read off the decay constant $f_{\rho(1700)} = 0.14 \text{ GeV}$ from the global minimum located at $\Lambda = 5.8 \text{ GeV}^2$. The associated coefficients in the polynomial expansion are modified into

$$\begin{aligned} b_0 &= 0.0106, & b_1 &= 0.0244, \\ b_2 &= 0.0031, & b_3 &= -0.0099, \end{aligned} \quad (29)$$

and the resultant behavior of the spectral density function $\rho^h(q^2)$ is displayed in Fig. 5(a). As expected, the spectral density function shifts further toward the large q^2 region with one more excited state being moved out of the continuum.

Motivated by the nontrivial U-shape minimum distribution in Fig. 10(a), we study next excited state. Adopting the spectral density,

$$\begin{aligned} \text{Im}\Pi(q^2) &= \pi f_\rho^2 \delta(q^2 - m_\rho^2) + \pi f_{\rho(1450)}^2 \delta(q^2 - m_{\rho(1450)}^2) \\ &\quad + \pi f_{\rho(1700)}^2 \delta(q^2 - m_{\rho(1700)}^2) \\ &\quad + \pi f_V^2 \delta(q^2 - m_V^2) + \pi \rho^h(q^2), \end{aligned} \quad (30)$$

we analyze the minimum distribution on the $\Lambda - m_V$ plane shown in Fig. 11(a), where the global minima located in the range $\Lambda \sim 6-7 \text{ GeV}^2$ give $m_V \sim 1.9 \text{ GeV}$. It is exactly the $\rho(1900)$ meson mass [24], implying that the third excited ρ state still emerges in our formalism. We then search the minimum distribution on the $\Lambda - f_V$ plane with m_V being set to $m_{\rho(1900)} = 1.9 \text{ GeV}$, namely, with the considered excited state being fixed to $\rho(1900)$. The global minimum in Fig. 11(b) located at $\Lambda = 7.1 \text{ GeV}^2$ gives the decay

constant $f_{\rho(1900)} = 0.14 \text{ GeV}$, which marks a prediction of our formalism that has not yet been attempted before. The corresponding coefficients in the polynomial expansion are

$$\begin{aligned} b_0 &= 0.0118, & b_1 &= 0.0242, \\ b_2 &= 0.0028, & b_3 &= -0.0095, \end{aligned} \quad (31)$$

and the resultant behavior of the spectral density function $\rho^h(q^2)$ is exhibited in Fig. 5(a).

One may wonder whether even higher excited ρ states can be probed in our formalism because some nontrivial U-shape minimum distribution still shows up in Fig. 11(a), with a small gap above the lower minimum distribution. Above $\rho(1900)$, there are $\rho(2150)$, which is a well-established state, and $\rho(2000)$, which is poorly established and needs confirmation [24]. We extend the parametrization in Eq. (30) to include one more unknown pole, with the other poles being fixed in the previous analysis. The scanning on the $\Lambda - m_V$ plane reveals the minimum distribution in Fig. 12. An obvious global minimum is located at $\Lambda \approx 7 \text{ GeV}^2$ with the corresponding mass $m_V \sim 2.0 \text{ GeV}$, which supports the existence of the $\rho(2000)$ state. Though

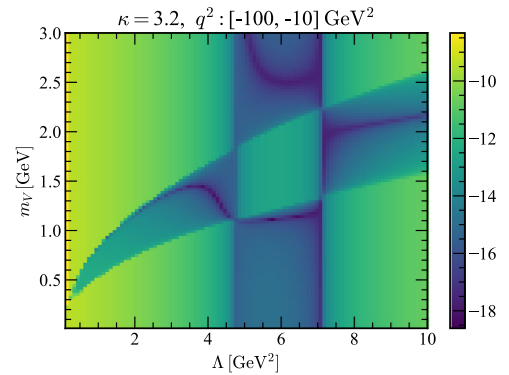


FIG. 12. Minimum distributions of RSS on the $\Lambda - m_V$ plane for the quintuple pole parametrization with $\kappa = 3.2$ and the input range $(-100 \text{ GeV}^2, -10 \text{ GeV}^2)$ in q^2 .

there is a vague U-shape minimum distribution above the tilted one, we will not proceed further the test application, and end the search of the excited ρ states here.

Our results for the decay constants of the $\rho(1450)$ and $\rho(1700)$ excitations are comparable to those derived in the literature, such as the sum rule analysis with nonlocal condensate corrections [5,10], the multiple pole QCD sum rules [11,33], the light cone quark model [34], the lattice QCD [35], and the rainbow-ladder truncation method [36]. The theoretical and experimental studies on the $\rho(1900)$ and higher states are still rare. Our formalism can be applied to the extraction of decay widths for excited ρ states in principle, which, however, demands more effort. Simply adding one more timelike pion form factor associated with $\rho(1450)$ to the $\rho(770)$ contribution, we observe no minimum distribution on the $\Lambda - \Gamma$ plane. This is not a surprise, since the $\pi^+\pi^-$ production in e^+e^- annihilation is basically saturated by the $\rho(770)$ intermediate resonance, and $\rho(1450)$ contributes little. At last, we make a remark on the maximum entropy method for sum rules. It is unlikely to reveal all the bound states simultaneously, especially when the mass spectrum becomes dense and multiple solutions exist for such an inverse problem. It may be possible to explore excited states using this method, if one follows our strategy: find the best fit solutions for excited states one by one. We will validate this conjecture in a future publication.

C. Sum rules with duality assumption

As an alternative viewpoint, the duality assumption in Eq. (10) can be regarded as an oversimplified parametrization with a single parameter s_0 for the spectral density in conventional sum rules. This simple parametrization with a step function satisfies the boundary conditions automatically: it vanishes at $s = 0$, and the duality assumption guarantees the continuity condition at $s = s_0$. Compared to our polynomial expansion, we have two free parameters, b_0 and b_1 . In this sense, our parametrization may be simple too but still more general than the duality assumption. We will

elaborate that one may not be able to explore properties of excited states reliably under the duality assumption. For the convenience of discussion, we present the version of Eq. (13) before the Borel transformation,

$$\frac{f_V^2}{m_V^2 - q^2} = \frac{1}{\pi} \int_0^{s_0} ds \frac{\text{Im}\Pi^{\text{pert}}(s)}{s - q^2} + \frac{1}{12\pi} \frac{\langle \alpha_s G^2 \rangle}{(q^2)^2} + 2 \frac{\langle m_q \bar{q}q \rangle}{(q^2)^2} + \frac{224\pi \kappa \alpha_s \langle \bar{q}q \rangle^2}{81 (q^2)^3}, \quad (32)$$

where the lower bound s_i in the integral on the right-hand side has been approximated by zero. The conventional sum rules in Eqs. (13) and (32) can also be handled as an inverse problem with the three unknowns m_V , f_V , and s_0 . This handling is basically the same as the best fit performed in [21], and more sophisticated than in [8,9], where the unknowns were solved by requiring the same asymptotic behavior for both sides of the sum rules, namely, by equating the coefficients of different powers in $1/q^2$ on both sides. We focus only on Eq. (32) and take the OPE from the range $(-100 \text{ GeV}^2, -10 \text{ GeV}^2)$ in q^2 as the input. It has been verified that results derived from the sum rule under the Borel transformation in Eq. (13) are the same.

The minimum distributions on the $s_0 - m_V$ and $s_0 - f_V$ planes for $\kappa = 3$ are presented in Figs. 13(a) and 13(b), respectively. The minimum distributions for $\kappa = 2$ and 4 are similar. It is found that there is only one minimum distribution on the $s_0 - m_V$, which increases monotonically with the threshold s_0 , like the lower minimum distribution in Fig. 6(a) attributed only to the perturbative piece of the OPE. Note that Fig. 4(a) contains two minimum distributions, where the lower one, corresponding to $m_V \approx 0.78 \text{ GeV}$, is stable with respect to the variation of Λ , and the upper one appears with a mass gap. The range of the threshold s_0 is supposed to be between $m_{\rho(770)}^2 \approx 0.6 \text{ GeV}^2$ and $m_{\rho(1450)}^2 \approx 2.2 \text{ GeV}^2$, within which neither a global minimum nor a plateau exists around the $\rho(770)$ meson mass. Certainly, one can choose an appropriate

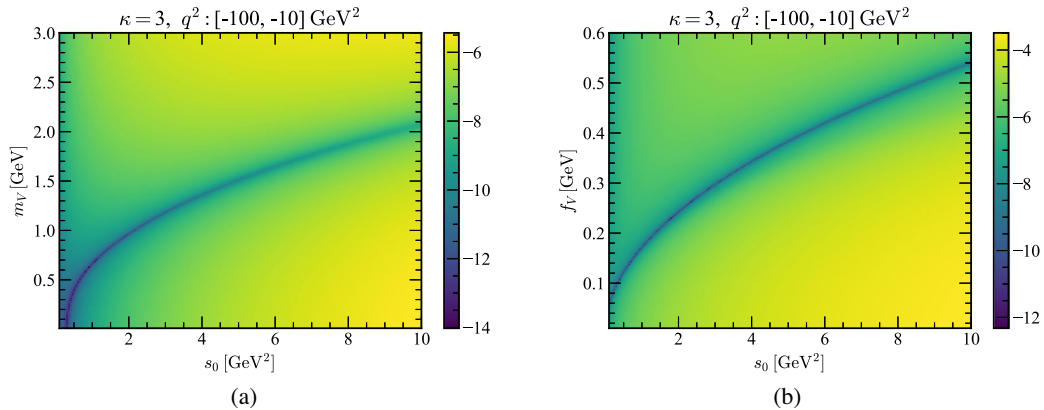


FIG. 13. Minimum distributions of RSS for the conventional sum rules under the duality assumption (a) on the $s_0 - m_V$ plane and (b) on the $s_0 - f_V$ plane with $\kappa = 3$ and the input range $(-100 \text{ GeV}^2, -10 \text{ GeV}^2)$ in q^2 .

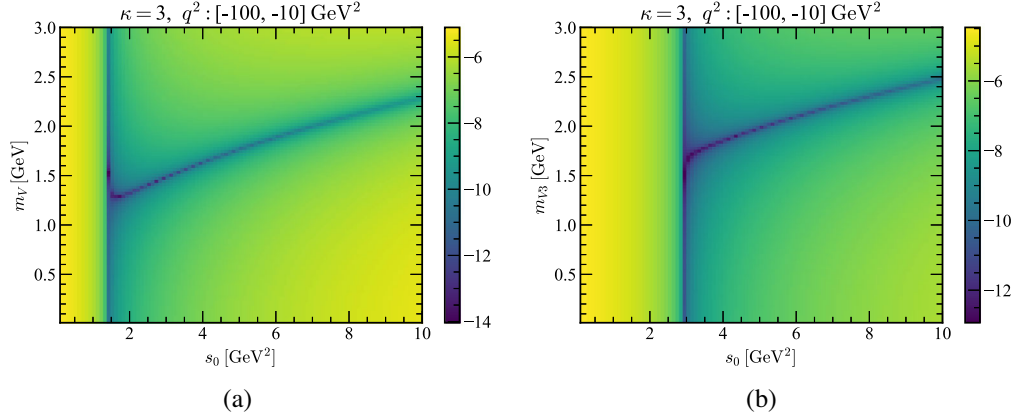


FIG. 14. Minimum distributions of RSS on the $s_0 - m_V$ plane for the conventional sum rules under the duality assumption (a) for the double pole parametrization, where the first pole is fixed to be $\rho(770)$, and (b) for the triple pole parametrization, where the second pole is further fixed to be $\rho(1450)$ with $\kappa = 3$ and the input range $(-100 \text{ GeV}^2, -10 \text{ GeV}^2)$ in q^2 .

s_0 value, say, $s_0 \approx 1.3 \text{ GeV}^2$ to get $m_V = 0.78 \text{ GeV}$. Then with this s_0 , one can read off $f_V = 0.2 \text{ GeV}$ from Fig. 13(b). In this sense, the conventional sum rules are less predictive but still useful for estimating the decay constant of the ground state, if its mass is fixed.

To check whether the conventional sum rule can probe the $\rho(1450)$ state, we apply the same strategy, solving the spectral density with a double pole parametrization, in which the ground state parameters are fixed to $m_{\rho(770)} = 0.78 \text{ GeV}$ and $f_{\rho(770)} = 0.2 \text{ GeV}$ read off above. Again, the $s_0 - m_V$ plane contains only one minimum distribution of RSS as shown in Fig. 14(a). In this case, a reasonable value of s_0 is supposed to be a bit higher than $m_{\rho(1450)}^2 \approx 2.1 \text{ GeV}^2$ and a bit lower than $m_{\rho(1700)}^2 \approx 2.9 \text{ GeV}^2$, as the finite widths of these excited states are taken into account. No global minimum, i.e., no reliable solution for a resonance, exists within this range, and results of m_V are always below the physical one $m_{\rho(1450)} \approx 1.46 \text{ GeV}$. The minimum at the lower bound of s_0 is deeper, but one has to push s_0 to the extreme $s_0 = 2.9 \text{ GeV}^2$ in order to barely reach $m_V = 1.46 \text{ GeV}$. The corresponding decay constant $f_V = 0.21 \text{ GeV}$, being larger than $f_{\rho(770)} = 0.2 \text{ GeV}$ of the ground state, is unlikely [11]. This is not a surprise because $s_0 = 2.9 \text{ GeV}^2$ is not a reasonable choice. If one insists on continuing to probe the next excited ρ state, the triple pole parametrization can be adopted, with the parameters of the second pole being further fixed to $m_{\rho(1450)} = 1.46 \text{ GeV}$ and $f_{\rho(1450)} = 0.21 \text{ GeV}$. The resultant minimum distribution on the $s_0 - m_V$ plane is exhibited in Fig. 14(b). It is seen that there is no global minimum, and all values of m_V in the designated range of $s_0 > (m_{\rho(1700)} + 0.1)^2 \approx 3.2 \text{ GeV}^2$ [11] with the finite width of $\rho(1700)$ being considered, are all greater than 1.7 GeV . Namely, no reliable and sensible solution is identified for the $\rho(1700)$ state.

The above investigation reveals clearly the limitation of conventional sum rules based on the duality assumption.

Though nontrivial minimum distributions of RSS still appear on the $s_0 - m_V$ plane, which are allowed by an ill-posed inverse problem, the duality assumption imposes too strong of a restriction on the shape of the continuum. It has to be a step function with the height being equal to that of the perturbative spectral density, and the threshold s_0 exists in a narrow interval. It means that the continuum has been roughly fixed, especially as excited states are probed, which are denser in the mass spectrum. Under this stringent restriction, solutions for resonances may not exist due to the absence of global minima and can hardly be correct, even as s_0 is stretched unreasonably. In summary, conventional sum rules may work for ground state studies, in which the interval of s_0 , namely, the flexibility of varying the continuum is bigger but should become unreliable for excited states.

IV. CONCLUSION

In this paper, we have improved QCD sum rules for nonperturbative studies without assuming the quark-hadron duality on the hadron side. The spectral density at low energy, including both resonance and continuum contributions, is solved with the OPE input on the quark side by treating sum rules as an inverse problem. We have elaborated the postulation that the Borel transformation is not crucial for this new formalism because the continuum contribution needs not to be suppressed but is solved via the inverse problem, and the convergence of the OPE is achieved by adopting the input in the deep Euclidean region. Once the unknown spectral density is solved directly, the stability criterion for conventional sum rules is not necessary either. The implementation of the above formalism has been demonstrated by identifying the series of ρ states and by determining their corresponding decay constants from the two-current correlator. The strategy is to include resonances one by one into the spectral density with different associated continuum contributions, and to repeat solving the sum rules by minimizing the difference between

the hadron and quark sides. One should make sure in the above procedure that the scale Λ , separating the perturbative and nonperturbative regimes, should be above the highest resonance parametrized into the unknown spectral density for consistency. In this way, we have predicted the decay constants $f_{\rho(770)}(f_{\rho(1450)}, f_{\rho(1700)}, f_{\rho(1900)}) \approx 0.22$ (0.19, 0.14, 0.14) GeV for the masses $m_{\rho(770)}(m_{\rho(1450)}, m_{\rho(1700)}, m_{\rho(1900)}) \approx 0.78$ (1.46, 1.7, 1.9) GeV of the ρ resonances. The decay width $\Gamma_{\rho(770)} \approx 0.17$ GeV of the $\rho(770)$ meson has been also obtained. We mentioned that the existence of the $\rho(1570)$ state could not be excluded, which has been speculated to be due to an Okubo-Zweig-Iizuka-suppressed decay mode of $\rho(1700)$, and that the existence of the $\rho(2000)$ state is supported.

The major sources of theoretical uncertainties arise from the OPE for the OPE inputs, which is truncated at finite orders in α_s and at finite powers of $1/q^2$. We have observed that the variation of the factorization violation parameter κ from 3 to 4 causes about 10% variation to the results presented in this work. More precise inputs, such as reliable κ values and condensates, help determine nonperturbative observables. Here, we have fixed κ to be 3.2 to produce the $\rho(770)$ meson mass. The dimension-eight condensates are still quite uncertain [16,37–39] and deserve more investigation. Second, the expansion of the spectral density function ρ^h in a series of Legendre polynomials is truncated at the fourth term. Though the convergence of this expansion has been scrutinized, the precision of our predictions can be improved by including higher order polynomials. When this is done, the continuity of the slope of the spectral density function at the separation scale can also be imposed, and its impact is worth investigation. It is claimed that both the above sources of theoretical uncertainties can be reduced straightforwardly and systematically. One may still question whether the separation scales

Λ about few GeV^2 in our study are large enough for justifying the replacement of the continuum contribution $\text{Im}\Pi(s)$ by the perturbative one $\text{Im}\Pi^{\text{pert}}(s)$, which is also based on the quark-hadron duality. Certainly, it is not the concerned duality assumption in conventional QCD sum rules around the threshold $s_0 \approx 1 \text{ GeV}^2$, and the duality violation above $\Lambda \approx \text{few GeV}^2$ is expected to be minor.

This new formalism is more predictive with less ambiguity and more control of theoretical uncertainty, compared to conventional sum rules because the unknown observables were extracted from the best fit of the two sides of a sum rule. In particular, it can be extended to analyses of excited states, which are difficult to achieve in conventional sum rules. We have observed that the condensate corrections up to dimension-six seem to be sufficient for generating most known ρ resonances. Since whether a bound state exists can be explored in our formalism, it would be of interest to apply it to the various exotic channels, such as those containing more than three quarks. It is worthwhile to generalize it to pursue nonperturbative properties of vector mesons in nuclear medium [40,41] at finite density or temperature to directly observe the change in the spectral density function in hot or dense environments. Our formalism cannot only be applied to low energy light flavor processes but also to heavy flavor physics [42–46]. It is also possible to extend it to studies of nonlocal condensate effects on excited states [5,10] and on other more complicated QCD processes [47–51]. There is no doubt that there are broad applications of our nonperturbative formalism.

ACKNOWLEDGMENTS

This work was supported in part by the Ministry of Science and Technology of R.O.C. under Grant No. MOST-107-2119-M-001-035-MY3.

-
- [1] M. A. Shifman, A. I. Vainshtein, and V. I. Zakharov, *Nucl. Phys.* **B147**, 385 (1979); **B147**, 448 (1979).
 - [2] C. Coriano and H. n. Li, *Phys. Lett. B* **324**, 98 (1994).
 - [3] D. B. Leinweber, *Ann. Phys. (N.Y.)* **254**, 328 (1997).
 - [4] P. Gubler and M. Oka, *Prog. Theor. Phys.* **124**, 995 (2010).
 - [5] A. Bakulev and S. Mikhailov, *Phys. Lett. B* **436**, 351 (1998).
 - [6] M. A. Shifman, A. I. Vainshtein, M. B. Voloshin, and V. I. Zakharov, *Phys. Lett. B* **77**, 80 (1978).
 - [7] V. A. Novikov, L. B. Okun, M. A. Shifman, A. I. Vainshtein, M. B. Voloshin, and V. I. Zakharov, *Phys. Rep.* **41**, 1 (1978); *Phys. Lett. B* **67**, 409 (1977).
 - [8] N. V. Krasnikov and A. A. Pivovarov, *Phys. Lett. B* **112**, 397 (1982); *Yad. Fiz.* **35**, 1270 (1982) *Sov. J. Nucl. Phys.* **35**, 744 (1982).
 - [9] N. V. Krasnikov, A. A. Pivovarov, and N. N. Tavkhelidze, *Z. Phys. C* **19**, 301 (1983).
 - [10] A. Pimikov, S. Mikhailov, and N. Stefanis, *Few Body Syst.* **55**, 401 (2014).
 - [11] M. Maior de Sousa and R. da Silva, *Braz. J. Phys.* **46**, 730 (2016).
 - [12] K. Ohtani, P. Gubler, and M. Oka, *Phys. Rev. D* **87**, 034027 (2013).
 - [13] Y. Chung, H. G. Dosch, M. Kremer, and D. Schall, *Z. Phys. C* **25**, 151 (1984).
 - [14] S. Narison, *Phys. Lett. B* **361**, 121 (1995).
 - [15] S. Narison, *Phys. Lett. B* **673**, 30 (2009).
 - [16] D. Boito, M. Golterman, M. Jamin, K. Maltman, and S. Peris, *Phys. Rev. D* **87**, 094008 (2013); D. Boito, A. Francis,

- M. Golterman, R. Hudspith, R. Lewis, K. Maltman, and S. Peris, *Phys. Rev. D* **92**, 114501 (2015).
- [17] M. Gonzalez-Alonso, A. Pich, and A. Rodriguez-Sanchez, *Phys. Rev. D* **94**, 014017 (2016).
- [18] Y. Kwon, M. Procura, and W. Weise, *Phys. Rev. C* **78**, 055203 (2008).
- [19] H. N. Li, H. Umeeda, F. Xu, and F. S. Yu, *Phys. Lett. B* **810**, 135802 (2020).
- [20] H. N. Li and H. Umeeda, *Phys. Rev. D* **102**, 094003 (2020).
- [21] Q. N. Wang, Z. F. Zhang, T. Steele, H. Y. Jin, and Z. R. Huang, *Chin. Phys. C* **41**, 074107 (2017).
- [22] S. Narison, *Nucl. Part. Phys. Proc.* **258–259**, 189 (2015).
- [23] R. Buchert and N. A. Papadopoulos, *Phys. Lett. B* **296**, 430 (1992).
- [24] M. Tanabashi *et al.* (Particle Data Group), *Phys. Rev. D* **98**, 030001 (2018).
- [25] W. Sun *et al.* (χ QCD Collaboration), *Chin. Phys. C* **42**, 063102 (2018).
- [26] Z. G. Wang and S. L. Wan, *Phys. Rev. C* **76**, 025207 (2007).
- [27] S. Bhatnagar and Shi-Yuan Li, *J. Phys. G* **32**, 949 (2006).
- [28] M. Blank, A. Krassnigg, and A. Maas, *Phys. Rev. D* **83**, 034020 (2011).
- [29] H. M. Choi and C. R. Ji, *Phys. Rev. D* **75**, 034019 (2007).
- [30] C. A. Dominguez and N. Paver, *Z. Phys. C* **31**, 591 (1986).
- [31] M. Fischer *et al.* (ETM Collaboration), arXiv:2006.13805.
- [32] A. Ahmadov, Y. L. Kalinovsky, and M. Volkov, *Int. J. Mod. Phys. A* **30**, 1550161 (2015); **33**, 1892002(E) (2018).
- [33] A. A. Pivovarov, *Phys. At. Nucl.* **62**, 1924 (1999).
- [34] D. Arndt and C. R. Ji, *Phys. Rev. D* **60**, 094020 (1999).
- [35] T. Yamazaki *et al.* (CP-PACS Collaboration), *Phys. Rev. D* **65**, 014501 (2001).
- [36] S. x. Qin, L. Chang, Y. x. Liu, C. D. Roberts, and D. J. Wilson, *Phys. Rev. C* **85**, 035202 (2012).
- [37] B. Blok and M. Lublinsky, *Phys. Rev. D* **57**, 2676 (1998).
- [38] M. Gonzalez-Alonso, A. Pich, and J. Prades, *Phys. Rev. D* **81**, 074007 (2010); **82**, 014019 (2010).
- [39] C. Dominguez, L. Hernandez, K. Schilcher, and H. Spiesberger, *J. High Energy Phys.* **03** (2015) 053.
- [40] T. Hatsuda and S. H. Lee, *Phys. Rev. C* **46**, R34 (1992).
- [41] S. Leupold, W. Peters, and U. Mosel, *Nucl. Phys. A* **628**, 311 (1998).
- [42] M. Neubert, *Phys. Rev. D* **45**, 2451 (1992).
- [43] P. Ball, V. M. Braun, and H. G. Dosch, *Phys. Rev. D* **48**, 2110 (1993).
- [44] V. Belyaev, A. Khodjamirian, and R. Ruckl, *Z. Phys. C* **60**, 349 (1993).
- [45] T. Huang, Z. H. Li, and C. W. Luo, *Phys. Lett. B* **391**, 451 (1997).
- [46] Y. b. Dai, C. s. Huang, M. q. Huang, H. Y. Jin, and C. Liu, *Phys. Rev. D* **58**, 094032 (1998).
- [47] S. V. Mikhailov and A. V. Radyushkin, *JETP Lett.* **43**, 712 (1986).
- [48] A. Grozin, *Int. J. Mod. Phys. A* **10**, 3497 (1995).
- [49] A. P. Bakulev, A. V. Pimikov, and N. G. Stefanis, *Phys. Rev. D* **79**, 093010 (2009).
- [50] R. C. Hsieh and H. n. Li, *Phys. Lett. B* **698**, 140 (2011).
- [51] N. G. Stefanis and A. V. Pimikov, *Nucl. Phys. A* **945**, 248 (2016).